Table I. Asymmetric Alkylation of β-Lactam Esters **1**

β-lactam ester[a]	alkyl bromide	base[b]	genertn of enolate I temp (°C)	genertn of enolate I time (min)	additn of RBr temp (°C)	additn of RBr time (h)	product	yield[c] (%)	stereoselctvty[d] (% de)
1a	CH_2=CH—CH_2Br	LDA	0	15	-78	5	**2a-1**	95	>98 (R)
1a	CH_2=CH—CH_2Br	LHDS	0	15	0-5	5	**2a-1**	94	95 (R)
1b	CH_2=CH—CH_2Br	LDA	-78	15	-78	5	**2b-1**	95	34 (S)
1a	$PhCH_2Br$	LDA	0	15	-78	5	**2a-2**	96	>98 (R)
1a	$PhCH_2Br$	LDA	0	15	0-5	5	**2a-2**	95	93 (R)
1a	$PhCH_2Br$	LDA	-10	15	-10	5	**2a-2**	93	75 (R)
1a	$PhCH_2Br$	LDA	-90	15	-90	5	**2a-2**	95	50 (R)
1b	C_2H_5Br	LDA	0	15	-78	5	**2b-3**	95	>98 (R)
1b	3,4-$(MeO)_2$-C_6H_4-CH_2Br	LDA	0	15	0-5	5	**2b-4**	95	93 (R)

[a] **1a** = (3*S*,4*R*)-isomer; **1b** = (3*R*,4*S*)-isomer. [b] LDA = lithium diisopropylamide; LHDS = lithium hexamethyldisilylamide. [c] Determined by ^{1}H NMR. Conversion yield for the reaction is >99% in every case. [d] Determined by ^{1}H NMR. No the other diastereomer was detected for the cases with >98% de. *R* or *S* in the parentheses is the configuration of the newly formed quaternary center.

Scheme III[a]

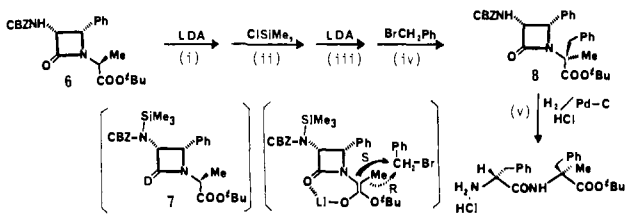

[a] (i) 1 equiv, THF, -78 °C, 3 min; (ii) 1 equiv, -78 → 0 °C, 75 min; (iii) 1 equiv, THF, 0 °C, 10 min, then cool to -78 °C; (iv) 3 equiv, -78 °C (2 h), -78 → 0 °C (3 h), 0 °C (2 h), then saturated NH_4Cl in MeOH; SiO_2 column; (v) 10% Pd-C, 1 N HCl (1 equiv), MeOH, 50 °C, 12 h.

THF at 110 °C gave the corresponding optically pure α-amino acid in good yield.[6]

In this asymmetric alkylation, we observed an interesting dependence of stereoselectivity on the reaction temperature as shown in Table I. When the reaction was carried out at -78 to -95 °C, the results of the alkylations were discouraging since the ratios of two diastereomers were only 2:1-3:1, and the enolate generated showed intense violet color. However, when the enolate was generated at 0-5 °C, the stereoselectivities of the alkylations were excellent, and the enolate generated exhibited yellow color.

Upon treatment with LDA or LHDS, a β-lactam ester, e.g., **1a**, should generate a chelating enolate I and/or a nonchelating enolate II. On the basis of the widely accepted transition-state model for the kinetic enolate formation, the nonchelating enolate II is favorable, when generated at -78 to -90 °C (Scheme II). Since the kinetic enolate cannot form a rigid chelate ring with the β-lactam oxygen by any means, it is reasonable that the stereoselectivity of the alkylation is low. The experiments at 0-5 °C imply that the thermodynamic enolate I which has a rigid chelate structure is generated at this temperature as originally designed and achieves excellent stereoselectivity. Thus, there is an isomerization process from the kinetic enolate II to the thermodynamic enolate I when the reaction is carried out at 0-5 °C. In fact, we observed a short-lived violet color at 0 °C when LDA in THF was added dropwise to a solution of β-lactam ester 1a in THF.

When 3-CBZ-NH-β-lactam ester **6** (CBZ = carbobenzyloxy) was employed as a substrate for the asymmetric alkylation, the reaction using 2 equiv of LDA and 1 equiv of benzyl bromide gave a poor result (ca. 20% de). This may indicate that the β-lactam oxygen cannot hold double coordination of lithium. Accordingly, chlorotrimethylsilane (TMS-Cl) was added after the addition of 1 equiv of LDA at -78 °C to form 3-CBZ-N(TMS)-β-lactam ester **7**, and then another 1 equiv of LDA was added at 0 °C followed by the addition of benzyl bromide at -78 °C. The stereoselectivity of this reaction was 14:1 as we expected (Scheme III). The hydrogenolysis of the alkylated β-lactam ester **8** on Pd-C gave (*R*)-(phenylalanyl)-(*S*)-2-methylphenylalanine *tert*-butyl ester hydrochloride in nearly quantitative yield.

Further studies on the application of this method to new double and triple asymmetric alkylations are actively in progress.

Acknowledgment. This research was supported by grants from the Center for Biotechnology, SUNY at Stony Brook, which is sponsored by the New York State Science and Technology Foundation and from National Institutes of Health (NIGMS). The generous support from Ajinomoto Co., Inc. is also gratefully acknowledged.

Supplementary Material Available: Procedures for the asymmetric alkylation of β-lactams and for the reductive cleavage of alkylated β-lactam esters, identification data for the alkylated β-lactam esters, the determination of absolute configurations, and a stereomodel of a lithium β-lactam ester enolate (5 pages). Ordering information is given on any current masthead page.

Catalysis by Human Leukocyte Elastase. 9. pH-Dependent Change in the Rate-Limiting Step[1,2]

Ross L. Stein*[3] and Anne M. Strimpler

Department of Pharmacology, Stuart Pharmaceuticals, a Division of ICI Americas Inc. Wilmington, Delaware 19897

Received June 12, 1987

We report that the rate-limiting step of k_c (see Scheme I and eq 1-4) for the HLE-catalyzed[4] hydrolyses of specific peptide *p*-nitroanilide substrates is dependent on pH and changes from acylation, at pH values less that 5.5, to deacylation, at pH values greater than 6.0.

$$k_c = \frac{k_2 k_3}{k_2 + k_3} \quad (1)$$

$$K_m = K_s \frac{k_3}{k_2 + k_3} \quad (2)$$

$$K_s = (k_{-1} + k_2)/k_1 \quad (3)$$

$$k_c/K_m = k_2/K_s = \frac{k_1 k_2}{k_{-1} + k_2} \quad (4)$$

pH dependencies for the HLE-catalyzed hydrolyses of four *p*-nitroanilides (Table I) indicate that while the pK_a for k_c/K_m

(1) For part 8 in this series, see ref 2.
(2) Stein, R. L.; Strimpler, A. M. *Biochemistry* **1987**, *26*, 2238-2242.
(3) Present address: Department of Enzymology, Merck Institute for Therapeutic Research, P.O. Box 2000, Rahway, NJ 07065.
(4) Abbreviations: HLE, human leukocyte elastase; MeOSuc, methoxysuccinyl; *p*NA, *p*-nitroanilide.

0002-7863/87/1509-6538$01.50/0

Table I. pH Dependence of Human Leukocyte Elastase Catalysis[a]

	$(k_c/K_m)_{lim}$	pK_a	$(k_c)_{lim}$	pK_a
Ac-Ala-Ala-Ala-*p*NA	0.86 ± 0.04	7.16 ± 0.10	0.69 ± 0.03	6.91 ± 0.05
Ac-Ala-Pro-Ala-*p*NA	2.67 ± 0.03	7.29 ± 0.02	1.62 ± 0.04	7.03 ± 0.09
Ac-Ala-Pro-Val-*p*NA	31.6 ± 0.06	7.21 ± 0.04	8.3 ± 0.2	6.23 ± 0.08
MeOSuc-Ala-Ala-Pro-Val-*p*NA[b]	295 ± 5	7.18 ± 0.04	13.6 ± 0.3	6.14 ± 0.05

[a] pH dependencies of kinetic parameters were determined as described previously.[9] In all cases, the pH was varied from 4 to 9. Units: k_c/K_m, $mM^{-1}\ s^{-1}$; k_c, s^{-1}. [b] Reference 9.

Scheme I

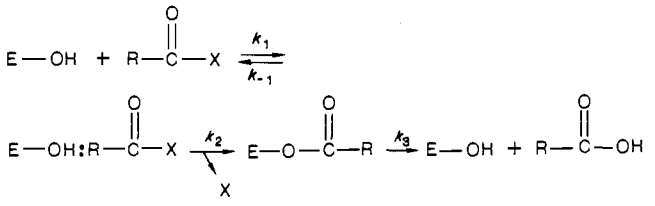

is independent of substrate structure and the magnitude of $(k_c/K_m)_{lim}$ (average value of $pK_a = 7.21 \pm 0.05$), values of pK_a for k_c display a negative correlation with $(k_c)_{lim}$; as $(k_c)_{lim}$ increases from 0.7 to 14 s^{-1}, pK_a decreases from 7.0 to 6.1.

These results suggest a mechanism for k_c involving a pH-dependent change in rate-limiting step. Such a mechanism is supported by previous studies[5-7] with *p*-nitroanilide substrates demonstrating that k_c becomes increasingly rate-limited by deacylation as peptide chain length and k_c increase.

To incorporate this new mechanistic feature, k_2 and k_3 of eq 1 were replaced by eq 5 and 6, respectively. In eq 5 and 6, $(k_2)_{lim}$

$$k_2 = \frac{(k_2)_{lim}}{1 + [H^+]/K_2} \quad (5)$$

$$k_3 = \frac{(k_3)_{lim}}{1 + [H^+]/K_3} \quad (6)$$

and $(k_3)_{lim}$ are the limiting values for k_2 and k_3 at high pH, and K_2 and K_3 are the acid dissociation constants of an ionizable amino acid residue that governs the pH dependencies of acylation and deacylation, respectively.[8]

Figure 1A contains the pH dependence of k_c for the HLE-catalyzed hydrolysis of MeOSuc-Ala-Ala-Pro-Val-*p*NA[9] and a curve constructed from the form of eq 1 in which k_2 and k_3 have been replaced by eq 5 and 6, respectively, and the parameters $(k_2)_{lim}$, pK_2, $(k_3)_{lim}$, and pK_3 have been set equal to the following: 170 s^{-1}, 7.1, 14 s^{-1}, and 5.8, respectively.[10] A fit of similar quality was obtained for Ac-Ala-Pro-Val-*p*NA with these parameters set to the following: 52 s^{-1}, 7.1, 11 s^{-1}, 5.8, respectively.[11]

Figure 1B contains theoretical pH dependencies for k_c, k_2, and k_3 for the pH dependence of the HLE-catalyzed hydrolysis of MeOSuc-Ala-Ala-Pro-Val-*p*NA and illustrates the pH-dependent change in the rate-limiting step. It can be seen that at low pH,

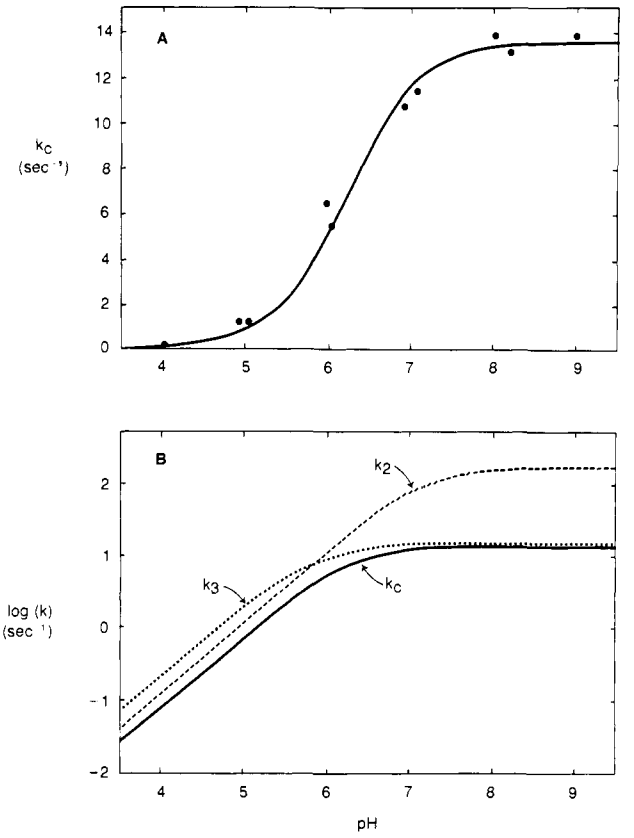

Figure 1. (A) Dependence of k_c on pH for the HLE-catalyzed hydrolysis of MeOSuc-Ala-Ala-Pro-Val-*p*NA. Data points were taken from ref 9. Solid line was drawn according to eq 1, 5, and 6 with $(k_2)_{lim}$, pK_2, $(k_3)_{lim}$, and pK_3 constrained to 170 s^{-1}, 7.1, 14 s^{-1}, and 5.8, respectively. (B) pH dependencies of k_c, k_2, and k_3 according to eq 1, 5, and 6 and the parameters given above.

k_c is rate-limited by acylation, whereas at high pH, k_c becomes rate-limited by deacylation. At pH values near 6, neither acylation nor deacylation entirely rate-limits k_c.[13]

pH-dependent changes in rate-limiting step are not uncommon in enzymology.[14-17] However, the work reported herein is a case in which the demonstration of this phenomenon is particularly clear. For the two most reactive substrates, we were able to unambiguously identify the partially rate-limiting steps as acylation and deacylation and then determine the extent to which these steps rate-limit k_c as a function of pH. In contrast, for Ac-Ala-Ala-Ala-*p*NA and Ac-Ala-Pro-Ala-*p*NA, k_c is entirely rate-limited by acylation over the entire pH range examined.

The changes in the rate-limiting step that we observe arise, in part, from an unusually low pK_a for the active site His in the acyl

(5) Stein, R. L.; Viscarello, B. R.; Wildonger, R. A. *J. Am. Chem. Soc.* **1984**, *106*, 796–798.
(6) Stein, R. L. *J. Am. Chem. Soc.* **1985**, *107*, 5767–5775.
(7) Stein, R. L.; Strimpler, A. M.; Hori, H.; Powers, J. C. *Biochemistry* **1987**, *26*, 1301–1305.
(8) Fersht, A. *Enzyme Structure and Function*, 2nd ed.; W. H. Freeman and Co.: New York, 1985; pp 155–175.
(9) Stein, R. L. *J. Am. Chem. Soc.* **1983**, *105*, 5111–5116.
(10) A nonlinear least-squares fit of the data of Figure 1 to eq 1 (after substitution of eq 5 and 6 for k_2 and k_3, respectively) did not converge. However, when $(k_3)_{lim}$ was constrained to 14 s^{-1} [this can be seen to be a reasonable upper limit for k_3 in ref 7] and pK_3 was constrained to 5.8 [this is consistent with data for hydrolysis of MeOSuc-Ala-Ala-Pro-Val-ONP by HLE given in ref 5], nonlinear least-squares fit provided values for $(k_2)_{lim}$ and pK_2 of 170 ± 23 s^{-1} and 7.1 ± 0.1, respectively.
(11) In fitting the pH dependence of k_c for the HLE-catalyzed hydrolysis of Ac-Ala-Pro-Val-*p*NA, pK_2 and pK_3 were assumed to be approximately the same as for the tetrapeptide substrate, and a value for $(k_3)_{lim}$ of 11 s^{-1} was taken from k_c for the hydrolysis of Ac-Ala-Pro-Val-OCH_3 at pH 9.[12] Nonlinear least-squares fit provided a value of $(k_2)_{lim}$ equal to 52 ± 8 s^{-1}.
(12) Stein, R. L.; Strimpler, A. M.; Wolanin, D. A., unpublished results.
(13) As one referee pointed out, our data can be successfully fit to eq 1 even if one of the two steps is assumed to be pH-dependent. While this is entirely correct, the pH dependence of both acylation and deacylation was based on what is known of serine proteases in general and HLE in particular.
(14) Fersht, A. R.; Requena, Y. *J. Am. Chem. Soc.* **1971**, *93*, 7079–7087.
(15) Stein, R. L.; Cordes, E. H. *J. Biol. Chem.* **1981**, *256*, 767–772.
(16) Cook, P. F.; Cleland, W. W. *Biochemistry* **1981**, *20*, 1979–1805, 1805–1816.
(17) Cleland, W. W. *Methods Enzymol.* **1982**, *87*, 390–405.

enzyme. The low pK_a is presumably caused by shielding of the His from bulk solvent. This is similar to the situation observed for papain in which the pK_a of active site His-159 is about 4 in derivatives of papain in which the negatively charged sulfur of Cys-25 is neutralized by acylation.[18] In native papain, the pK_a of His-159 is near 8.[18]

(18) Johnson, F. A.; Lewis, S. D.; Shafer, J. A. *Biochemistry* **1981**, *20*, 44-48.

NMR Solvent Peak Suppression with a Soft-Pulse Nonlinear Excitation Sequence

Malcolm H. Levitt*

Francis Bitter National Magnet Laboratory
Massachusetts Institute of Technology
Cambridge, Massachusetts 02139

James L. Sudmeier and William W. Bachovchin

Tufts University School of Medicine
Boston, Massachusetts 02111
Received March 23, 1987

Considerable effort has gone into designing NMR radio-frequency pulse sequences that suppress a strong but unwanted resonance by avoiding its excitation.[1-11] The best-known applications for these frequency-selective excitation sequences involve ^1H NMR studies of the H_2O-exchangeable protons of nucleic acids and proteins. Here alternative methods for reducing the H_2O signal, such as saturation by selective preirradiation or use of ^2H_2O as a solvent, fail because they also reduce or eliminate the signals of interest.

The frequency response of an ideal solvent peak suppression sequence would show a flat region of minimal excitation close to the H_2O signal, flanked by broad bands of maximal excitation free from frequency-dependent phase variations. This combination of properties is elusive. For example, the "jump-return" pulse sequence[2] gives good phase behavior, but the range of suppression is narrow and the excitation bands are not flat. The popular 1331 sequence[4,5] gives a broad suppression band but delivers maximal excitation over a relatively narrow band of frequencies, with considerable phase variations. Recent suggestions increase the excitation bandwidths but induce even larger phase gradients.[6-10]

It has recently been shown[11] that a frequency response close to the ideal can be attained by taking advantage of the nonlinear response obtained with large flip angles. The new class of sequences is called NERO (nonlinear excitation rejecting on-resonance). In initial trials,[11] difficulty was encountered in solutions of high H_2O concentration, for reasons still not entirely clear. We now demonstrate that this is not an inherent property of the NERO pulse sequences by reporting good solvent peak suppression in aqueous solution together with flat excitation free from phase gradients. We also present a new member of this class, NERO-2

$$(48)-\overline{110}-(115)-\overline{130}-240-(360)-240-\overline{130}-(115)-\overline{110}-(48) \quad \text{(I)}$$

which is a time-symmetric sequence of six rectangular pulses and five delays of free precession, the latter given by the intervals in parentheses. Overbars indicate pulses 180° out of phase. This soft-pulse sequence is used by adjusting the radio-frequency field intensity such that the Rabi frequency is twice the frequency difference between the solvent resonance and the center of the desired excitation band. Pulse durations are then calculated as usual in terms of the flip angles given above. The precession delays in parentheses have been given as rotating-frame precession angles at the center of the excitation band—therefore, in this case, the time units are twice those of the pulses. The delay at the beginning of the sequence is only necessary when the sequence is used in combination with other pulses, in which case NERO-2 behaves just as a single 90° pulse about the x axis for those spins within the excitation bands.

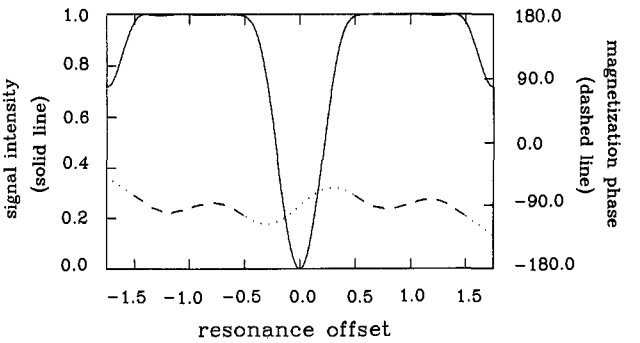

Figure 1. Theoretical frequency dependence of the intensity (solid line) and phase (dashed line) of transverse magnetization excited by NERO-2. The frequency units are normalized to the offset between solvent null and excitation band midpoint.

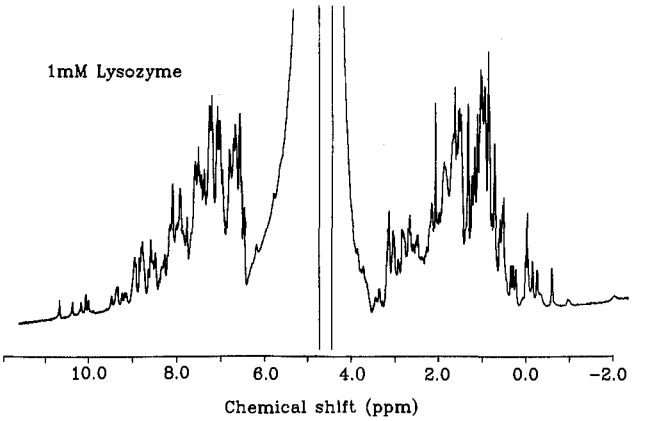

Figure 2. 400-MHz proton spectrum of 1 mM hen egg-white lysozyme in 90% H_2O and 10% ^2H_2O at 57 °C obtained in 100 transients on a Bruker AM-400 with NERO-2. The pulse sequence intervals in (I) were 76.3, (159.7), 90.2, 166.7, (500.0), 166.7, 90.2, (159.7), 76.3, and (66.7) μs in chronological order (precession delays in parentheses, initial delay omitted). The "trim pulse" had a duration of 3 μs.

Figure 1 illustrates the theoretical performance of NERO-2, as predicted by numerical simulation of the Bloch equations in the absence of relaxation. The excited frequency bands are symmetric with respect to the solvent "notch" and are wide and flat, with the phase of excited transverse magnetization varying by only ±15°. These phase variations may be reduced further if different phases on either side of the solvent peak are acceptable, as shown elsewhere. Sequences based on linear response with comparable excitation bandwidths[6-10] have a similar overall duration, but they produce a phase difference of about 450° across the same range.

Figure 2 shows an experimental 400-MHz proton spectrum of a 1 mM solution of lysozyme in 90% H_2O and 10% ^2H_2O. The Bruker AM-400 spectrometer was modified by incorporation of a digital phase synthesizer to improve the accuracy of the phase shifts. The 180° pulse duration was 125 μs, thereby giving maximal excitation of frequency bands between 2.5 and 7.5 ppm upfield or downfield from water. The suppression of the water peak was satisfactory (about 300:1), and a large number of exchangeable NH proton resonances are visible. There are no

(1) Redfield, A. G.; Kunz, S. D.; Ralph, E. K. *J. Magn. Reson.* **1975**, *19*, 114.
(2) Plateau, P.; Guéron, M. *J. Am. Chem. Soc.* **1982**, *104*, 7310.
(3) Sklenář, V.; Starčuk, Z. *J. Magn. Reson.* **1982**, *50*, 495.
(4) Turner, D. L. *J. Magn. Reson.* **1983**, *54*, 146.
(5) Hore, P. J. *J. Magn. Reson.* **1983**, *55*, 283.
(6) Gutow, J. H.; McCoy, M.; Spano, F.; Warren, W. S. *Phys. Rev. Lett.* **1985**, *55*, 1090.
(7) Starčuk, Z.; Sklenář, V. *J. Magn. Reson.* **1986**, *66*, 391.
(8) Morris, A.; Smith, K. A.; Waterton, J. C. *J. Magn. Reson.* **1986**, *68*, 526.
(9) Hall, M. P.; Hore, P. J. *J. Magn. Reson.* **1986**, *70*, 350.
(10) Wang, C.; Pardi, A. *J. Magn. Reson.* **1987**, *71*, 154.
(11) Levitt, M. H.; Roberts, M. F. *J. Magn. Reson.* **1987**, *71*, 576.

0002-7863/87/1509-6540$01.50/0